Comparative study of Coral Conversion, Part 2: Microstructural evolution of calcium phosphate

Innocent J. Macha[1], Upsorn Boonyang[2], Sophie Cazalbou[3], Besim Ben-Nissan[1], Cedric Charvillat[3], Faik N Oktar[4] and David Grossin[3]

1) Department of Chemistry and ForensicScience, University of Technology Sydney, Broadway NSW 2007
2) School of Science, Walailak University, 222 Thaiburi, Thasala District, Nakhonsithammarat, 80160 Thailand.
3) CIRIMAT Carnot Institute, University of Toulouse, UPS-INPT-CNRS UMR 5085, France
4) Department of Bioengineering, Faculty of Engineering, University of Marmara, Kadikoy 34722, Istanbul, Turkey.

Email: innocent.macha@uts.edu.au

Available at: www.austceram.com/ACS-Journal

Abstract
Calcium phosphate materials can be easily produced by a number of wet chemical methods that involve both acidic and basic environments. In our previous study, we investigated calcium phosphates such as monetite, hydroxypatite and whitlockite which were successfully produced by mechano-chemical method from corals obtained from the Great Barrier Reef. It was observed that a number of synthesis factors such as the pH of the environment, the reaction temperature and the chemistry influenced the crystal size formed. A number of theories have been suggested on the mechanisms of crystal formation; however, very few mechanisms have been universally accepted. The present work was aimed to explore the evolution of crystalline calcium phosphate and their morphology with respect to the pH of the environment and reaction time. Conversion of coral to calcium phosphates was carried out with stoichiometric amount of required H_3PO_4 or $(NH_4)_2HPO_4$, to obtain hydroxyapatite (HAp) or tri calcium phosphate (TCP) phases. The acidic or basic solution was added, drop wise, at a rate of 2 mL min^{-1}, to 6 g of coral powder suspended in 300 mL of distilled water at 80 ± 0.5°C on a hot plate with magnetic stirrer. The pH of reaction was monitored. Crystal morphology and the phases were identified by XRD, FTIR, and SEM studies. It was observed that under acidic conditions (H_3PO_4), dissolution and then precipitation influences the crystal morphology and transition from plate like to rod like hydroxyapatite structure. During the first hour of the dissolution a monetite and hydroxyapatite mixture precipitates and then the full conversion to hydroxyapatite is observed. However under basic conditions ($(NH_4)_2HPO_4$), pH is only marginally changed within the environment and just surface conversion of the calcium carbonate structure of coral to hydroxyapatite and a very small amount of tri-calcium phosphate is observed. The mechanism can be classified as the solid state topotactic ion-exchange reaction mechanism.

Keywords: Hydroxyapatite, calcium phosphate, pH, Mechano-chemical conversion, morphology.

1. Introduction

Hydroxyapatite ($Ca_{10}(PO_4)_6(OH)_2$, HAp) is one of the main inorganic structures in calcified tissues. Because of its biocompatibility and osteoconductive properties, it has been extensively investigated for dental and orthopaedic medical applications (1, 2). In addition, hydroxyapatite is also used in many other applications such as in cosmetics, as tooth paste additions, in chromatography, in protein purification and water treatment (3-5). Various production and synthesis methods of HAp have been proposed, for example, hydrothermal (6-10), sol-gel (11-13), microwave irradiation (14-16), and precipitation (17-19). Among them, the most popular process for the HAp synthesis is the wet chemistry aqueous dissolution method that could be easily executed and is inexpensive (19-21). The mechanism of mechano-chemical process was explained in a number of previous publications (19, 20).

In our previous study, calcium phosphate materials such as monetite, hydroxypatite and whitlockite were successfully produced by mechano-chemical method from corals (19). Two convenient conditions of acidic and basic environments were studied. Boskey and Posner stated that precipitation of calcium phosphate

 ISSN 0004-881X

from a system which contains total calcium and phosphate each with a concentraion higher than 10 milimoles per liter (mmol.l^{-1}) and at pH values greater than 6.8, the precipitation is always preceded by the formation of an amorphous precursor, hydroxyapatite (HAp) $Ca_5(PO_4)_3OH$ (22). Their theory is very much consistence with the Ostwald Rule of Stages in Precipitation (23). It was postulated that in this process there is tranformation of precipitates through some intermediate states to the thermodynamically stable product, HAp crystal. Supersaturation, pH values, impurities like magnesium, strontium are some of the factors influence these transformations (24, 25). Shimoda and his colleagues reported that, carbonate ions, are growth inhibitors for the apatitic structure (26). They found that these ions tend to substitute anions in biological apatites which affect morphological and structural features of carbonated calcium apatites. Rey et al found that carbonate environment in bone-mineral enhanced IR shift of carbonate and stabilizes the non-apatitic surface layer present on apatite nanocrystals (27). Theories have been suggested on the mechanisms of crystal formation, however, only a very few mechanisms have been globally accepted. Final morphologies and structures observed from these transformations not clearly explained.

The present work, aims to explore the evolution of crystalline calcium phosphate and their morphologies with respect to different pH environments and under different reaction times.

2. Materials and Methods

Coral is a living animal and like all living things unfortunately suffers from many environmental factors and its inorganic component fosilises. In this current research like in our all previous research no living corals were used. Coral fosilised skeletons causes and Corals were obtained from two different sources; one from the Great Barrier Reef, QLD Australia and the second one from artificially grown corals from Prof. R. Vago of the Ben-Gurion University of Negev, Israel. The methods of coral pre-preparation were covered in our previous publications. Diammonium hydrogen phosphate ($(NH_4)_2HPO_4$, 98%), hydrophosphoric acid (H_3PO_4, 85%) and sodium hypochlorite (NaClO) were obtained from Sigma Aldrich (Castle Hill, Australia).

2.2 Methods

2.2.1 Conversion of coral to calcium phosphates

Coral samples were prepared following the procedures shown in an earlier paper (28). The amount of $CaCO_3$ and the thermal decomposition products of coral was determined using TG/DTA method described in (19). Conversion of coral to calcium phosphates materials followed the following procedures. Stoichiometric amount required of H_3PO_4 or $(NH_4)_2HPO_4$, (to obtain HAp or TCP), was dissolved in 25 ml of deionised water. Then the mixture was added, drop wise, at a rate of 2 mL min^{-1}, to 6 g of coral powder in 300 mL of distilled water at 80 ± 0.5°C on a hot plate with magnetic stirrer. The reaction vessel was covered to prevent evaporation. The reaction was kept under stirring (270 rpm) for 24 hrs. After dropping all phosphate solutions in the mixture, pH of reaction mixture was monitored every 5 min during the first 30 min, every 30 min for 3 hrs and every hour for 7 h. 5 mL of reaction mixture was pipetted at every pH measuring point, then solids were separated by centrifuging (Eppendorf, Centrifuge 5702) for 1 min at 4400 rpm. The solids were washed triple time with 18 MΩ (MilliQ, Millipore, Victoria, Australia) water and separated by centrifuge, then dried overnight in an oven at 80 ± 0.1°C for further analysis. The reactant solutions were prepared from analytical grade reagents.

The methods aimed to convert corals to HAp by using H_3PO_4 and $(NH_4)_2HPO_4$ were coded HA-P and HA-A, respectively. The ones aimed to convert corals to TCP by using H_3PO_4 and $(NH_4)_2HPO_4$ were coded TCP-P and TCP-A, respectively. Samples HA-P were taken for 30, 60, 90,120, 150, 180, 240, 300, 360, 420 min and 24 hrs were coded HA-P1, HA-P2, HA-P3, HA-P4, HA-P5, HA-P6, HA-P7, HA-P8, HA-P9, HA-P10 and HA-P11, respectively.

2.2.2. Phase analysis by XRD

Phase analysis of the products were carried out by X-ray powder diffraction using D8 ADVANCE (BRUKER), radiation Cu Kalpha1+2 = 0.15418 nm, no monochromator, from 20 to 80° (2 theta), steps of 0.02°, 2 seconds/step, divergence slit 0.3°, Sollers slit 2.5°, detector linear: LynxEye (2.73°) The phase quantification was done using Rietveld analysis performed by Topaz software and crystal size was determined by Scherer with Topaz software.

2.2.3 Morphology by SEM

The SEM pictures were taken with a Zeiss Supra 55VP SEM with RAITH E-beam Lithography System & EBSD for the secondary electron imaging (SEI) the energy was kept at 20 kV, working distance and magnification were varied to obtain best possible pictures. The powder samples were fixed by mutual conductive adhesive tape on aluminium stubs and coated with carbon using a sputter coater (CEA 010, Balzers union FL-9496 Balzers, SCD 020).

2.2.4 FTIR analysis

The synthesized calcium phosphate powders were ground in an agate mortar and thoroughly mixed with KBr (FTIR Grade). Three milligrams of powder sample was mixed with 300 mg of KBr powder (1% w/w). Transparent pellets were prepared in a stainless steel die by applying a uniaxial load of 6.89 MPa pressure (Carver press). The FTIR spectra were collected using a Nicolet, Magna-IR 6700 Spectrometer FTIR (Thermo Fisher Scientific, Madison USA) in the range 2200–400 cm^{-1}.

3. Results and Discussions

3.1 Results

3.1.1 pH Measurements

During the reaction time pH was regularly measured for all experiments and the results are presented in Figure 1. It can be seen that during the first 180 minutes for H_3PO_4 additions the pH changes from 3.6 to 6.3, while in $(NH_4)_2HPO_4$ additions the pH changes marginally only from 7.3 to 7.6. For 24 hrs period the same trend is observed for both HA and TCP. For TCP experiments there is little fluctuation of pH from the beginning of experiment to the end.

3.1.2 FTIR

The chemical structures of the synthesis products evolved in the first 3 hours of reactions for all experiments and after 24 hours were analysed by FTIR and presented in Figure 2. The conversion of coral to calcium phosphates seemed to start immediately after addition of the reactants and mixing the pre-cursor at 80 ^oC. In all three experiments, after 30 minutes of reaction FTIR could detect characteristic vibrations of PO_4 and vibration and absorption peaks for calcite which is the main component in coral. For HA-A and HA-P these vibration occur at 575 and 561 cm^{-1}, correspond to ($\nu_4 PO_4$ of HAp), 945 cm^{-1} ($\nu_1 PO_4$ of β-TCP), 575 and 561 cm^{-1} ($\nu_4 PO_4$ of HAp) for TCP-A and TCP-P. The presence of calcite after 30 minutes is attributed by the absorption band around 876 cm^{-1} which corresponds to ν_3CO_3 vibration mode and the absorption band of weak intensity around 1417 cm^{-1} correspond to symmetrical and asymmetrical stretching modes of the ν_3CO_3 groups (C-O) (29).

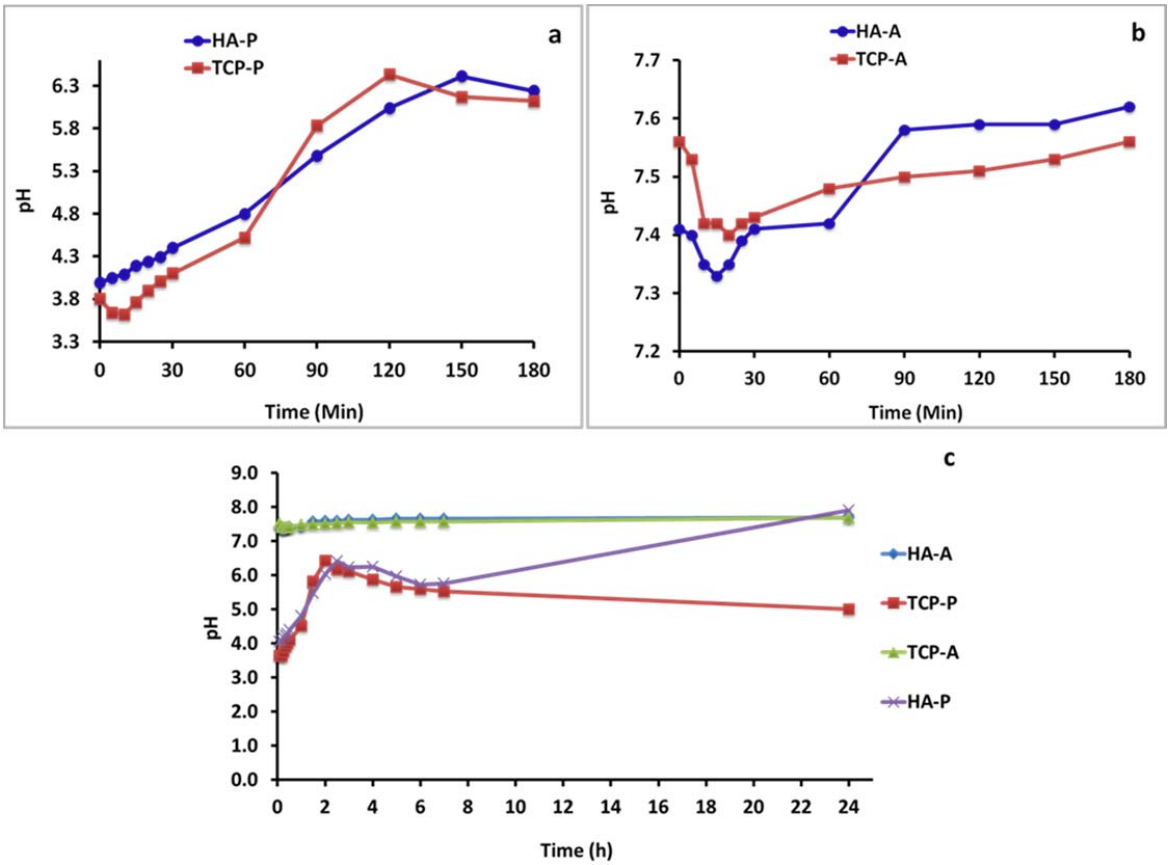

Figure 1: Change of pH of the reaction mixture **a**) Phosphoric acid and corals, the first 3 hrs **b**) Diammonium hydrogen phosphates and corals, the first 3 hrs **c**) Both a&b mixtures for 24 hrs.

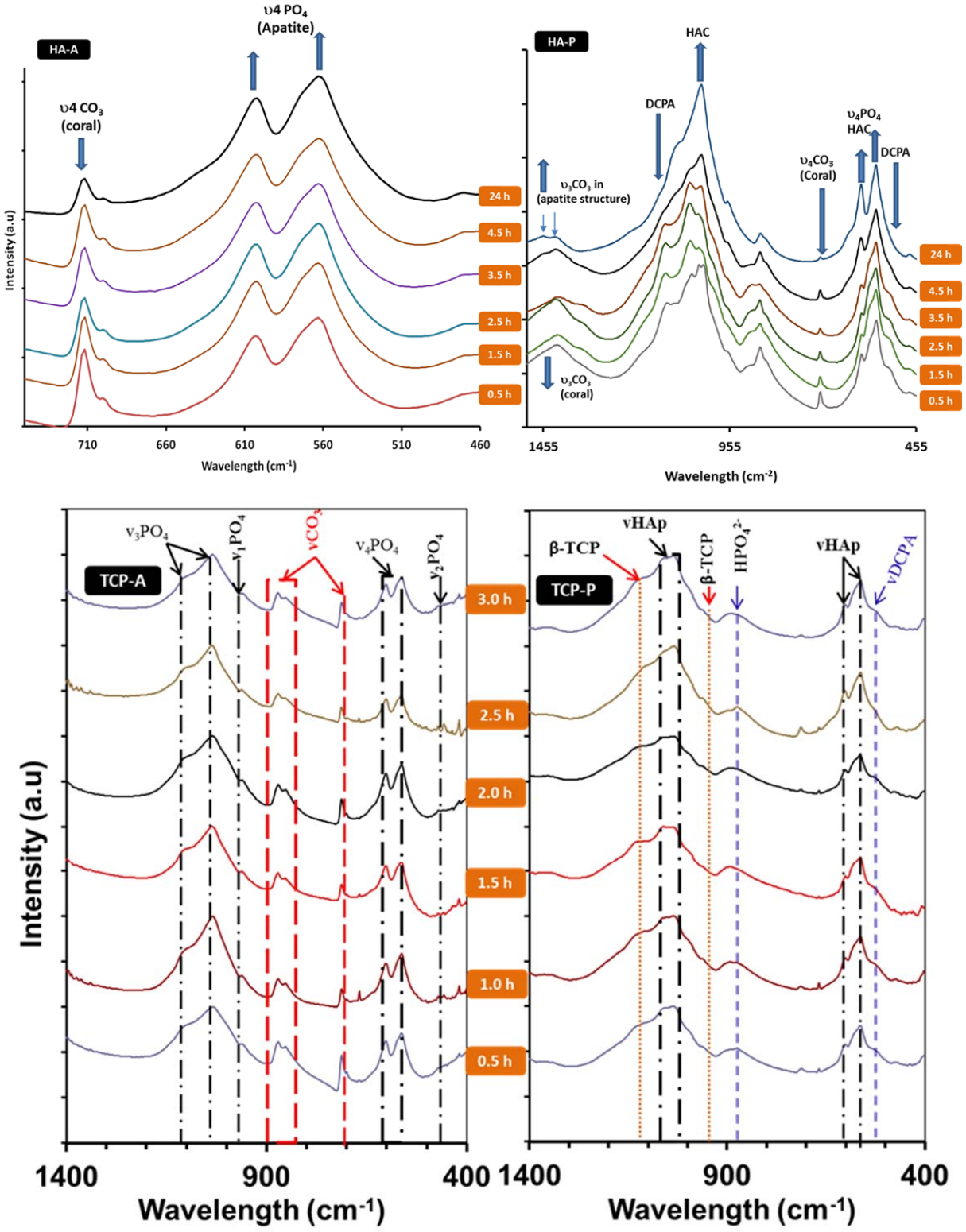

Figure 2: FTIR spectra of experimental products, sampling after every 30 minutes for the first 3 hrs and after 24hrs of the conversion process of; Coral to HAp using $(NH_4)_2HPO_4$-HA-A, Coral to HAp using H_3PO_3 –HA-P, Coral to TCP by using $(NH_4)_2HPO_4$ –TCP-A and Coral to TCP by using H_3PO_3-TCP-P

Absorption band at 712 cm^{-1} is due to the in-plane bending mode of v_4CO_3. Absorption maximum of CO_3 group at 876 cm^{-1} can also suggest that AB-type PO_4 and OH groups substitution in the structure of HAp. The microstructural evolution of calcium phosphate materials from these reaction happened with time and both FTIR and XRD results suggested that some of the calcium phosphates formed in the beginning of the reaction were intermediate products which is consistence with SEM results. After 24 hrs of reactions, Figure 2 shows FTIR spectra of the four experimental samples. It is suggested that the products that formed in the first half an hour are still present after 24 hours.

3.1.3 XRD

The intermediate products like monetite for HA-P experiments was consumed during the process and remained in small quantity according to XRD results shown in Table 1. On the other hand direct conversion of HAp from calcite/aragonite was observed as XRD results suggested in Table 2 for HAp-A experiments.

The Table 1 clearly demonstrates the amounts of monotite and hydroxyapatite mixture formation as an initial reaction at the earlier stages of the acid addition and then the increase of HAp phase as a function of time. The results also suggest that with increased reaction time, the HAp crystallites grew from 40 to approximately to 80 nm within 24 hrs under the acidic environment.

Table 2 demonstrates the transformation of coral to hydroxyapatite under $(NH_4)_2HPO_4$, HAp-A experiments. Original structure and retained phases shows that the coral is a mixture of aragonite-calcite mixture and main conversion is to the hydroxyapatite phase. The initial amount of 28% HAp increases to 53% after 24 hour period while in comparison the HAp-P after 24 hrs showed 82% conversion. Crystal growth seems like did not occur but crystal sizes stayed around 50-60nm.

Table 1: Quantification for HA-P experiment showing the amount of precipitated phases and growth of HAp phase

Time (h)	Aragonite (%)	Calcite (%)	Monetite (%)	TCP beta (%)	HAp (%)	Size 002 Scherer (nm)
0.5	4.4±0.4	24.4±0.3	29.0±0.3	0.9±0.2	41.4±0.5	42
1.0	2.8±0.3	19.4±0.2	38. ±0.31	0.8±0.1	38.8±0.4	61
1.5	2.6±0.2	16.8±0.2	42.8±0.3	1.2±0.1	36.6±0.3	58
2.0	2.5±0.3	14.8±0.2	48.8±0.3	1.5±0.1	32.4±0.3	53
3.0	2.5±0.2	16.0±0.2	43.7±0.3	2.3±0.1	35.5±0.3	61
4.0	1.5±0.2	13.3±0.2	40.7±0.3	3.2±0.1	41.3±0.3	62
5.0	1.3±0.2	12.5±0.2	31.8±0.2	4.7±0.1	49.9±0.3	72
7.0	0.9±0.2	9.6±0.2	24.5±0.2	5.8±0.2	59.2±0.3	82
24.0	0.3±0.1	7.2±0.1	0.6±0.1	7.2±0.1	84.8±0.4	77

Table 2: Quantification for HA-A experiment showing the amount of transformed phases crystal growth of HAp

Time (h)	Aragonite (%)	Calcite (%)	HAp (%)	Size 002 Scherer (nm)
0.5	13.6±0.6	48.4±0.6	38.0±0.5	53
1.0	13.0±0.5	49.2±0.6	37.8±0.6	61
1.5	12.3±0.5	48.0±0.6	39.7±0.6	54
2.0	12.2±0.5	48.6±0.5	39.2±0.6	51
3.0	11.5±0.5	46.5±0.5	42.0±0.6	53
4.0	11.5±0.5	47.4±0.5	41.0±0.6	48
5.0	11.4±0.4	44.4±0.5	44.2±0.5	56
7.0	10.9±0.4	44.6±0.5	44.5±0.5	52
24.0	7.5±0.3	33.5±0.3	58.9±0.4	53

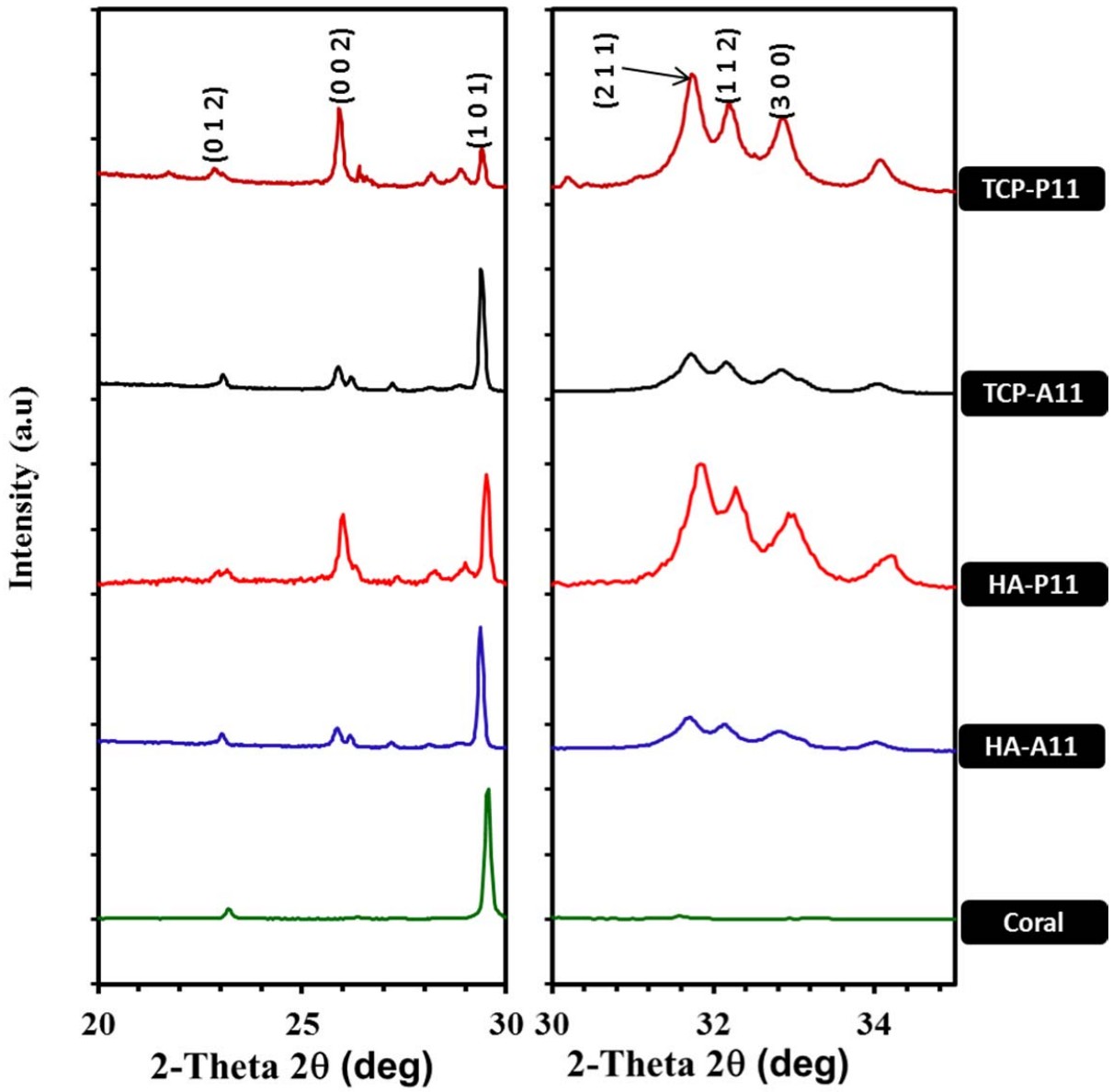

Figure 3: XRD patterns of samples after 24 hrs

Figure 3 shows the XRD results after 24 hrs of reaction for four different reactions. In all experiments for HAp-P XRD patterns present small phase of raw materials suggesting that the reaction was nearly completed during the 24 hrs period. However the HAp-A showed around 50% coral not converted after 24 hrs period. Interestingly, all products from ammonium phosphate solution reactions (HA-A&TCP-A) have the hydroxyapatite (HAp) crystal structure with just a very minute amount of other phases of calcium phosphate is detected. However the reaction involving orthophosphoric phosphate acid solution has HAp with other calcium phosphate compounds like whitlockite (minor phase) and monetite for HA-P and monetite for TCP-P.

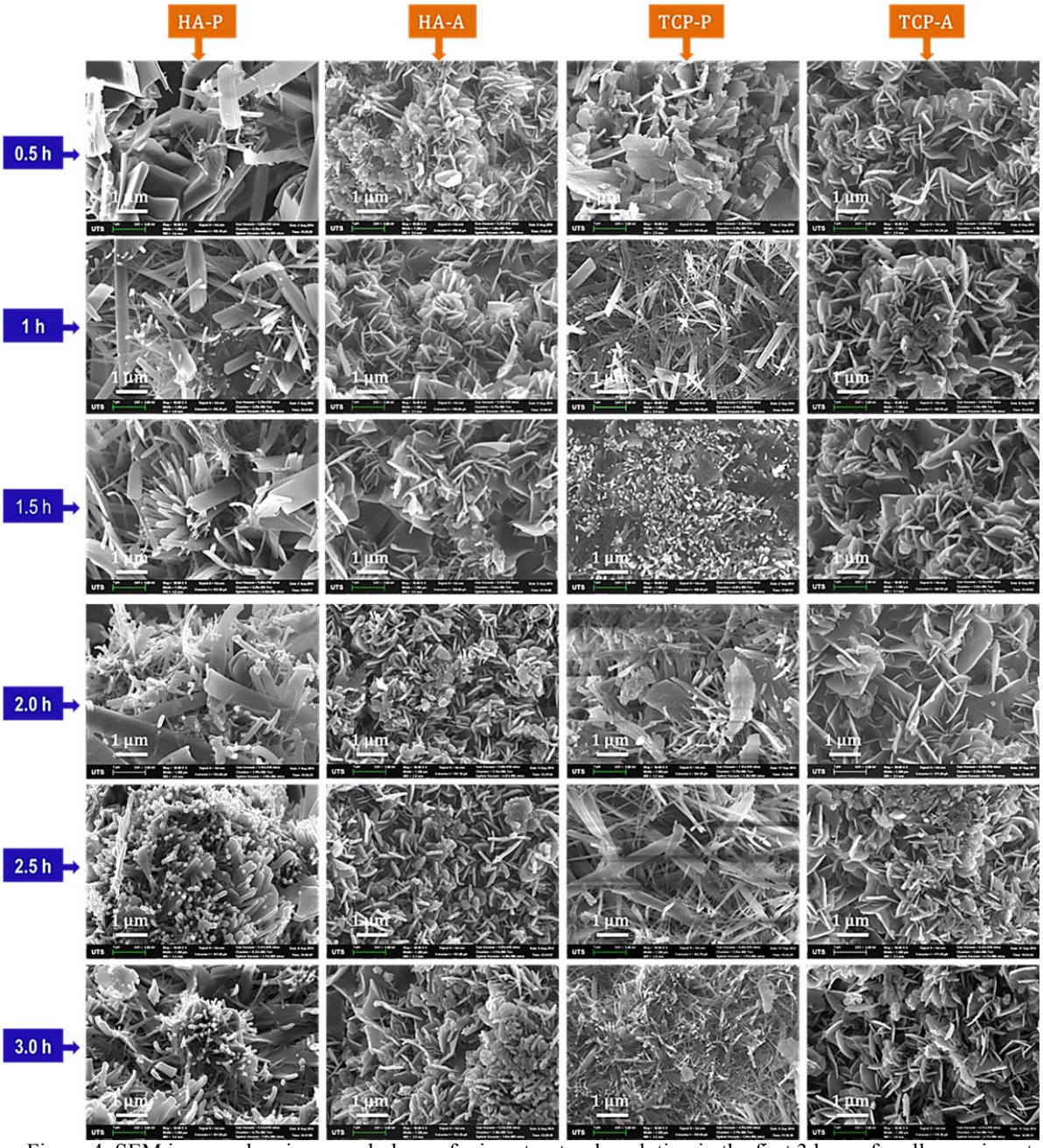

Figure 4: SEM images showing morphology of microstructural evolution in the first 3 hours for all experiments.

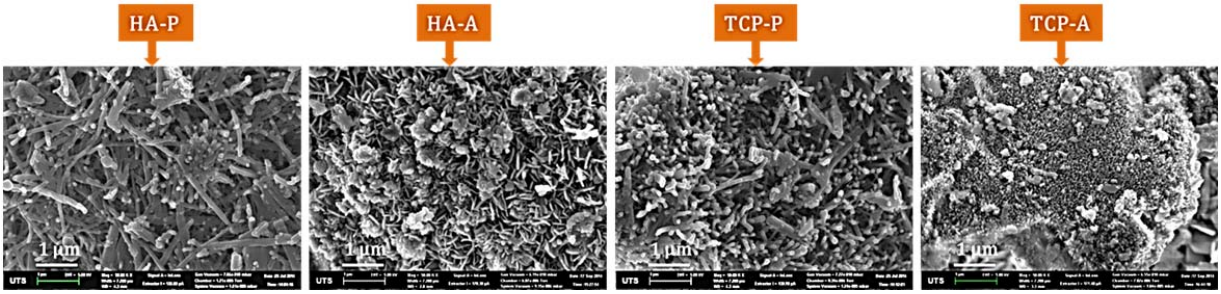

Figure 5: SEM images showing morphology experimental products after 24 hours of reaction.

3.1.4 Morphology

The morphology of calcium phosphate microstructural evolution presented in Figure 4 shows similarities between reaction under orthophosphoric phosphates solution (HA-P and TCP-P) as well as under ammonium phosphate solution (HA-A and TCP-A). The results revealed the morphology change with respect to time from platelets to rod-like morphology for reactions under orthophosphoric acid solution. With ammonia phosphate solution the morphologies for both HA-A and TCP-A are platelets similar to original unconverted coral suggesting the solid state topotactic ion-exchange reaction mechanism. On the other hand, when compared with orthophosphoric phosphate solution the reaction mechanism is suggested to be dissolution and recrystallization.

4. Discussions

This current work demonstrates the evolution of crystalline calcium phosphate materials from wet chemical conversion of coral structure with respect to time and pH. The observed morphology of products from conversion of coral in ammonium phosphate solution suggests that the method could help to retain the original coral structure, specifically the micro pores that are pertinent in bone graft or scaffolding applications and nano and mesopores for slow drug delivery applications. For ammonium phosphate solution, HAp crystalline evolution took place on the surface of platelets morphology of aragonite/calcite without changing the original morphology. While with orthophosphoric acid the observed morphology indicate the evolution (and growth) of rod-like morphology.

The crystal growth results for HA-P experiment suggest that HAp crystal size grew at the expense of monetite crystallise, which is consistence with the morphology observed in Figure 5. The results suggest that the transformation of monetite to hydroxyapatite or whitlockite via monetite route, involves a dissolution-recrystallization mechanism.

The reaction mechanism and final products are influenced by pH. The effect of pH on the reaction mechanisms and products can be further explained using classic solubility isotherms (Figure 6).

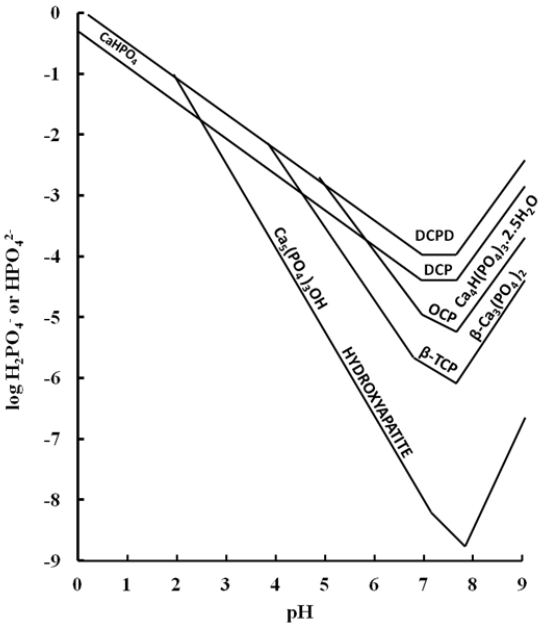

Figure 6: Solubility isotherms for differing calcium phosphate forms versus pH.

4.1 Orthophosphoric acid phosphate solution

For orthophosphoric acid phosphate solution reactions, pH seems to change in the beginning from 7.0 to 4.0 immediately after the addition of the acid and then it starts to continuously increase to 6.5 during the first 2 hrs period as shown in Figure 1 (a). As stated above during that period, of the addition of acid, pH drops immediately to around 3.8- 4.0. At this some point part of a "defect HAp" initially formed (The HAp formed is calcium deficient or "defect HAp") and further coral dissolves in acidic condition and introduce further Ca^{2+} in to the environment to form monetite ($CaHPO_4$) (which is more stable at this point as shown in Figure 6). $CaHPO_4$ is one of the mildly acidic calcium phosphates and its amount increases within the solution (30). The release of PO_4 from dissolution of some of the initial "defect" HAp under increased acidity and phosphate ions generated from the acid and Ca^{2+} from dissolution of $CaCO_3$ induces the precipitation of further monetite. During the following period, some of the $CaCO_3$ continue to dissolve to counterbalance the acidic solution and this will increase the pH observed in Figure 1 to 6.5 during the first 2 hrs period.

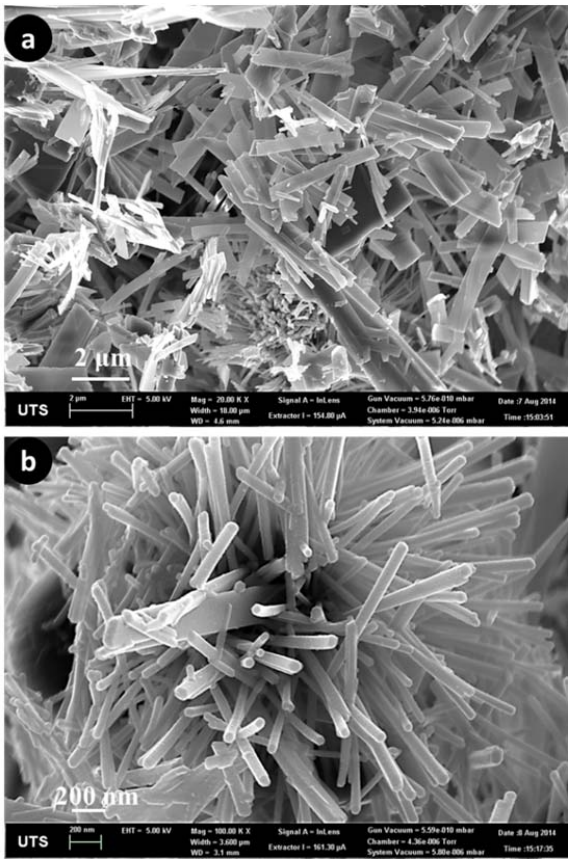

Figure 7: Morphology change from platelets (a) to rod-like (b) in 24 hrs

After 2 hours pH is around 6.2 and according to Figure 6, HAp is more stable and monetite formed earlier transforms to HAp and HAp starts to increase in the amounts as shown in Table 1, from. 50% to approximately 80%. Crystal sizes were measured using (002) reflections and Scherrer-Topaz method. Dissolution products from monetite, participate in the formation of additional HAp in which CO_2 and H_2O formation counter balance the decrease in pH due to HAp formation. This process is confirmed by the increase of HAp crystalline sizes shown in Table 1 and the change of morphology from platelet Figure 7a to rod like structures Figure 7b.

4.2 Ammonium phosphate solution

Under ammonium phosphate solution environment, pH starts to increase from around 7 before dropping marginally. The formation of HAp starts immediately as the first drop is added into the solution. Since the formation of HAp results into decrease in pH due to the formation of HCO_3^-, a sudden drop and then increase of pH is observed. After this initial position pH is well balanced and increase is observed with the addition of ammonium solution which is basic. pH condition in this transformation favours formation of HAp which is more stable at this pH compared to precursors like monetite (Figure 6). Similar behaviour in plate like hydroxyapatite formation and related morphological changes, it was suggested that the reaction mechanism in this conditions based on the "solid state topotactic ion-exchange reaction mechanism" (31).

5. Conclusion

In this study coralline materials convert to calcium phosphate compounds, such as HAp, monetite and whitlockite under moderate conditions of temperature. Two conversion routes were observed, first, solid state topotactic ion-exchange reaction mechanism using ammonium phosphate solution which mainly produce HAp and the second, dissolution-recrystallization using orthophosphoric acid phosphate solution which resulted into DCPA, HAp and whitlockite phases. Microstructural analysis showed platelike morphologies of coralline structures is changed to rod like structures under acidic condition by dissolution precipitation mechanism while under basic conditions the transformation to HAp does not influence the crystal shape or morphologies but some growth according to reaction time is observed. It is believed that during that time period, the addition of acid and the dissolution of calcium carbonate from coral and the reactions with the phosphatic ions within the environment interact to create the initial required reaction with Ca^{2+} ions to form preliminary monetite and HAp. According to Figure 6 in the first instance monetite will be stable and with the extra addition of acid, the pH will be further reduced to allow the initial HAp to be formed. It can be concluded that the reaction time and pH influence reaction mechanism and microstructure evolution. Production of HAp under basic or acidic conditions provides the possibility of controlling the defined morphology of calcium phosphates produced by controlling the pH and the reaction time.

References

1. **Chung E.J, Kodali P, Laskin W, Koh J.L, Ameer G.A.** Long-term in vivo response to citric acid-based nanocomposites for orthopaedic tissue engineering. Journal of materials science Materials in medicine. Vol.[**22**], 9, (2011), 2131-2138.
2. **Wang M.** Surface Modification of Biomaterials and Tissue Engineering Scaffolds for Enhanced Osteoconductivity. In: Ibrahim F, Osman N, Usman J, Kadri N, editors. 3rd Kuala Lumpur International Conference on Biomedical Engineering 2006. IFMBE Proceedings. 15: Springer Berlin Heidelberg; 2007. p. 22-27.

3. **Suen R.B, Lin S.C, Hsu W.H.** Hydroxyapatite-based immobilized metal affinity adsorbents for protein purification. Journal of chromatography A. Vol.[**1048**], 1, (2004), 31-39.
4. **Schlatterer B, Baeker R, Schlatterer K.** Improved purification of beta-lactoglobulin from acid whey by means of ceramic hydroxyapatite chromatography with sodium fluoride as a displacer. Journal of chromatography B, Analytical technologies in the biomedical and life sciences. 2004;Vol.[**807**], 2, (2004), 223-228.
5. **Christoffersen J, Christoffersen MR, Larsen R, Møller I.J.** Regeneration by surface-coating of bone char used for defluoridation of water. Water Research. Vol.[**25**], 2, (1991), 227-229.
6. **Andrés-Vergés M, Fernández-González C, Martínez-Gallego M.** Hydrothermal synthesis of calcium deficient hydroxyapatites with controlled size and homogeneous morphology. Journal of the European Ceramic Society. Vol.[**18**], 9, (1998), 1245-1250.
7. **Chou J, Ben-Nissan B, Choi A.H, R. Wuhrer, D. Green.** Conversion of coral sand to calcium phosphate for biomedical applications. Journal of the australian ceramic society. Vol.[**43**], 1, (2007), 5.
8. **Zhang F, Zhou Z.H, Yang S.P, Mao L.H, Chen H.M, Yu X.B.** Hydrothermal synthesis of hydroxyapatite nanorods in the presence of anionic starburst dendrimer. Materials Letters. Vol.[**59**], 11, (2005), 1422-1425.
9. **Ioku K, Kawachi G, Sasaki S, Fujimori H, Goto S.** Hydrothermal preparation of tailored hydroxyapatite. J Mater Sci. Vol.[**41**], 5, (2006), 1341-1344.
10. **Boonyang U, Chaopanich P, Wongchaisuwat A, Senthongkaew P, Siripaisarnpipat S.** Effect of Phosphate Precursor on the Production of Hydroxyapatite from Crocodile Eggshells. Journal of Biomimetics, Biomaterials and Tissue Engineering. Vol.[**5**], (2010), 7.
11. **Montazeri N, Jahandideh R, Biazar E.** Synthesis of fluorapatite–hydroxyapatite nanoparticles and toxicity investigations. International journal of nanomedicine. Vol.[**6**], (2011), 197-201.
12. **Fathi MH, Hanifi A.** Evaluation and characterization of nanostructure hydroxyapatite powder prepared by simple sol–gel method. Materials Letters. Vol.[**61**], 18, (2007), 3978-3983.
13. **Liu D-M, Troczynski T, Tseng W.J.** Water-based sol–gel synthesis of hydroxyapatite: process development. Biomaterials. Vol.[**22**], 13, (2001), 1721-1730.
14. **Murugan R, Ramakrishna S.** Production of ultra-fine bioresorbable carbonated hydroxyapatite. Acta Biomater. Vol.[**2**], 2, (2006), 201-206.
15. **Parhi P, Ramanan A, Ray A.R.** Synthesis of nano-sized alkaline-earth hydroxyapatites through microwave assisted metathesis route. Materials Letters. Vol.[**60**], 2, (2006), 218-221.
16. **Wang X, Fan H, Xiao Y, Zhang X.** Fabrication and characterization of porous hydroxyapatite/β-tricalcium phosphate ceramics by microwave sintering. Materials Letters. Vol.[**60**], 4, (2006), 455-458.
17. **Hongquan Z, Yuhua Y, Youfa W, Shipu L.** Morphology and formation mechanism of hydroxyapatite whiskers from moderately acid solution. Materials Research. Vol.[**6**], (2003), 111-115.
18. **Monmaturapoj N.** Nano-size Hydroxyapatite Powders Preparation by Wet-Chemical Precipitation Route. Journal of Metals, Materials and Minerals. Vol.[**18**], 1, (2008), 6.
19. **Cegla R-NR, Macha I.J, Ben-Nissan B, Grossin D, Heness G, Chung R-J.** Comparative Study of Conversion of Coral with Ammonium Dihydrogen Phosphate and Orthophosphoric Acid to Produce Calcium Phosphates. Journal of the Australian Ceramics Society. Vol.[**50**], 2, (2014), 154-1561.
20. **Macha I.J, Ozyegin L.S, Oktar F.N, Ben-Nissan B.** Conversion of Ostrich Eggshells (Struthio camelus) to Calcium Phosphates. J Aust Ceram Soc. Vol.[**51**], 2, (2015), 125-133.
21. **Macha I.J, Ozyegin L.S, Chou J, Samur R, Oktar F.N, Ben-Nissan B.** An Alternative Synthesis Method for Di Calcium Phosphate (Monetite) Powders from Mediterranean Mussel (Mytilus galloprovincialis) Shells. Journal of The Australian Ceramic Society. Vol.[**49**], 2, (2013), 122-128.
22. **Boskey A.L, Posner AS.** Formation of hydroxyapatite at low supersaturation. The Journal of Physical Chemistry. Vol.[**80**], 1, (1976), 40-45.
23. **Feenstra T.P, De Bruyn P.L.** The ostwald rule of stages in precipitation from highly supersaturated solutions: a model and its application to the formation of the nonstoichiometric amorphous calcium phosphate precursor phase. Journal of Colloid and Interface Science. Vol.[**84**], 1, (1981), 66-72.
24. **Kibalczyc W, Christoffersen J, Christoffersen M.R, Zielenkiewicz A, Zielenkiewicz W.** The effect of magnesium ions on the precipitation of calcium phosphates. J Cryst Growth. Vol.[**106**], 2-3, (1990), 355-366.
25. **Boskey A.L, Posner AS.** Conversion of amorphous calcium phosphate to microcrystalline hydroxyapatite. A pH-dependent, solution-mediated, solid-solid conversion. The Journal of Physical Chemistry. Vol.[**77**], 19, (1973), 2313-2317.

26. **Shimoda S, Aoba T, Moreno E.C, Miake Y.** Effect of solution composition on morphological and structural features of carbonated calcium apatites. Journal of dental research. Vol.[**69**], 11, (1990), 1731-1740.
27. **Hina A.** Etude de la réactivité en milieu aqueux, d'apatites phosphocalciques d'intérêt biologique Toulouse France: Toulouse, INPT; 1996.
28. **Macha I.J, Cazalbou S, Ben-Nissan B, Harvey KL, Milthorpe B.** Marine structure derived calcium phosphate-polymer biocomposites for local antibiotic delivery. Marine drugs. Vol.[**13**], 1, (2015), 666-6680.
29. **Barinov S.M, Rau J.V, Cesaro S.N, Ďurišin J, Fadeeva I.V, Ferro D, et al.** Carbonate release from carbonated hydroxyapatite in the wide temperature rage. Journal of Materials Science: Materials in Medicine. Vol.[**17**], 7, (2006), 597-604.
30. **Elmore K.L, Farr T.D.** Equilibrium in the System Calcium Oxide–Phosphorus Pentoxide–Water. Industrial & Engineering Chemistry. Vol.[**32**], 4, (1940), 580-586.
31. **Milev A, Kannangara G.S.K, Ben-Nissan B.** Morphological Stability of Plate-Like Hydroxyapatite. Key Engineering Materials. Vol.[**240-242**], (2003), 481-484.